



Since January 2020 Elsevier has created a COVID-19 resource centre with free information in English and Mandarin on the novel coronavirus COVID-19. The COVID-19 resource centre is hosted on Elsevier Connect, the company's public news and information website.

Elsevier hereby grants permission to make all its COVID-19-related research that is available on the COVID-19 resource centre - including this research content - immediately available in PubMed Central and other publicly funded repositories, such as the WHO COVID database with rights for unrestricted research re-use and analyses in any form or by any means with acknowledgement of the original source. These permissions are granted for free by Elsevier for as long as the COVID-19 resource centre remains active.



Brequinar and dipyridamole in combination exhibits synergistic antiviral activity against SARS-CoV-2 *in vitro*: Rationale for a host-acting antiviral treatment strategy for COVID-19

James F. Demarest^a, Maryline Kienle^a, RuthMabel Boytz^b, Mary Ayres^c, Eun Jung Kim^d, J.J. Patten^b, Donghoon Chung^d, Varsha Gandhi^c, Robert A. Davey^b, David B. Sykes^e, Nadim Shohdy^a, John C. Pottage Jr.^a, Vikram S. Kumar^{a,*}

^a Clear Creek Bio, Cambridge, MA, USA

^b NEIDL, Boston University, Boston, MA, USA

^c Department of Experimental Therapeutics, MD Anderson Cancer Center, Houston, TX, USA

^d University of Louisville, Louisville, KY, USA

^e Center for Regenerative Medicine, Massachusetts General Hospital, Boston, MA, 02114, USA

ARTICLE INFO

Keywords:

Brequinar

Dipyridamole

Dihydroorotate dehydrogenase (DHODH)

COVID-19

SARS-CoV-2

ABSTRACT

The severe acute respiratory syndrome coronavirus 2 (SARS-CoV-2) is the causative agent of coronavirus disease 2019 (COVID-19) and the associated global pandemic resulting in >400 million infections worldwide and several million deaths. The continued evolution of SARS-CoV-2 to potentially evade vaccines and monoclonal antibody (mAb)-based therapies and the limited number of authorized small-molecule antivirals necessitates the need for development of new drug treatments. There remains an unmet medical need for effective and convenient treatment options for SARS-CoV-2 infection. SARS-CoV-2 is an RNA virus that depends on host intracellular ribonucleotide pools for its replication. Dihydroorotate dehydrogenase (DHODH) is a ubiquitous host enzyme that is required for *de novo* pyrimidine synthesis. The inhibition of DHODH leads to a depletion of intracellular pyrimidines, thereby impacting viral replication *in vitro*. Brequinar (BRQ) is an orally available, selective, and potent low nanomolar inhibitor of human DHODH that has been shown to exhibit broad spectrum inhibition of RNA virus replication. However, host cell nucleotide salvage pathways can maintain intracellular pyrimidine levels and compensate for BRQ-mediated DHODH inhibition. In this report, we show that the combination of BRQ and the salvage pathway inhibitor dipyridamole (DPY) exhibits strong synergistic antiviral activity *in vitro* against SARS-CoV-2 by enhanced depletion of the cellular pyrimidine nucleotide pool. The combination of BRQ and DPY showed antiviral activity against the prototype SARS-CoV-2 as well as the Beta (B.1.351) and Delta (B.1.617.2) variants. These data support the continued evaluation of the combination of BRQ and DPY as a broad-spectrum, host-acting antiviral strategy to treat SARS-CoV-2 and potentially other RNA virus infections.

1. Introduction

As of July 2022, over 6 million deaths and 500 million cases of coronavirus disease 2019 (COVID-19), caused by the severe acute respiratory syndrome coronavirus 2 (SARS-CoV-2), have been reported worldwide (WHO 2022). The number of infections likely exceeds the number of reported cases with an estimated excess mortality of 18.2 million (Wang et al., 2022). Despite the availability of multiple prophylactic vaccines, SARS-CoV-2 continues to evolve, compromising the

efficacy of vaccines and monoclonal antibody (mAb)-based treatment options. Only a few small-molecule antivirals are available, including two RNA-dependent RNA polymerase (RdRp) inhibitors, remdesivir and molnupiravir, and one inhibitor of the SARS-CoV-2 main protease (Mpro), nirmatrelvir (which requires the pharmacologic booster ritonavir to achieve sufficient plasma drug levels). Accordingly, a high unmet medical need remains for safe, efficacious, and patient-friendly treatments for COVID-19.

While approved small molecules are direct-acting antivirals (DAAs)

* Corresponding author

E-mail address: brq@clearcreekbio.com (V.S. Kumar).

<https://doi.org/10.1016/j.antiviral.2022.105403>

Received 20 May 2022; Received in revised form 28 July 2022; Accepted 23 August 2022

Available online 28 August 2022

0166-3542/© 2022 Elsevier B.V. All rights reserved.

that target viral proteins, an alternative strategy is to use host-acting antivirals (HAAs) that target host pathways essential for the viral life-cycle. HAAs may provide advantages over DAAs including (a) broad-spectrum antiviral activity against several families of RNA viruses, and (b) a higher barrier to the development of resistance as host-targets typically remain unchanged in contrast to those virus mutations that lead to DAA resistance.

Dihydroorotate dehydrogenase (DHODH), a host enzyme essential for *de novo* pyrimidine synthesis, is emerging as a candidate target of HAAs. Brequinar (BRQ) is an orally available, selective, and potent low nanomolar human DHODH inhibitor (DHODHI) that depletes intracellular uridine, cytidine, and thymidine levels *in vitro* and *in vivo* (Peters et al., 1990, 1992; Sykes et al., 2016). As an antiviral, DHODHIs such as BRQ block the host production of cellular pyrimidine nucleoside triphosphates (NTPs) required by viruses for replication (Adcock et al., 2017; Bonavia et al., 2011; Park et al., 2020; Qing et al., 2010). To date, the BRQ clinical experience consists of multiple human clinical studies in more than 1000 subjects with viral infection, hematologic malignancies, or autoimmune disorders (Clear Creek Bio data on file; Joshi et al., 1997; Madak et al., 2019; Peters et al., 1992, 1990).

DHODHIs exhibit potent *in vitro* activity against several RNA viruses such as SARS-CoV-2, influenza, Zika (ZKV), Dengue (DENV), respiratory syncytial virus (RSV), and Ebola (EBOV) (Adcock et al., 2017; Bonavia et al., 2011; Park et al., 2020; Qing et al., 2010). Despite this promising *in vitro* data, the successful translation of DHODHI monotherapy showing clinical benefit is lacking. While the DHODHI NITD-982 exhibited *in vitro* antiviral activity against DENV, the *in vivo* treatment of infected mice had no effect on viremia (Wang et al., 2011). This is

likely due to the salvage pathways that can compensate for the reduction of pyrimidine NTPs by DHODH (Cuthbertson et al., 2020; Karle et al., 1980). The concentration of extracellular uridine in mammalian plasma may range up to 10 μM (Karle et al., 1980) and may have contributed to limited clinical efficacy of DHODH inhibition in the oncology setting (Peters et al., 1990).

A combination of DHODH and nucleotide salvage pathway inhibitors may therefore be required for optimal therapeutic efficacy (Fig. 1). Consistent with this hypothesis, the antiviral activity of a DHODHI against DENV was enhanced by the addition of cyclopentenyl uracil, an inhibitor of uridine salvage (Liu et al., 2020). Host nucleoside transporters, such as equilibrative nucleoside transporters (ENTs), facilitate the transport of extracellular pyrimidines. Dipyridamole (DPY), an ENT1/2/4 inhibitor, synergizes with BRQ in colon and pancreatic cancer cells (Cuthbertson et al., 2020). DPY, FDA approved in 1961 (FDA, 2022), also inhibits platelet aggregation and has widespread clinical use in combination with aspirin for the secondary prevention of stroke (AGGRENOX® USPI 2012). We evaluated the *in vitro* pharmacologic and antiviral activity of the combination of BRQ and DPY (BRQ + DPY) in uninfected and SARS-CoV-2-infected A549/ACE2 cells.

2. Materials and methods

2.1. Test articles

Brequinar (Selleck Chemicals, Cat# S6626) and dipyridamole (Sigma Aldrich Prod# D9766) were provided by Clear Creek Bio. Uridine (99% purity) was obtained from Sigma (Cat#: U3003-5G) and Alfa

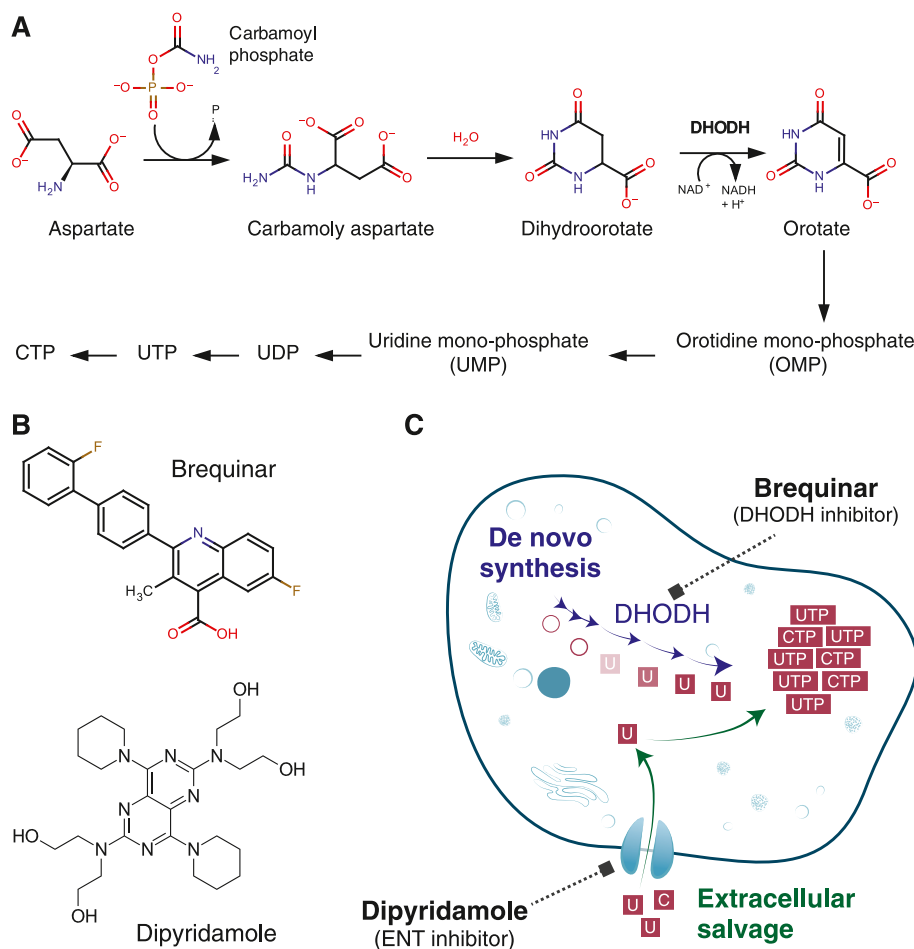


Fig. 1. A) *De novo* biosynthesis of pyrimidines. B) Structures of brequinar (BRQ) and dipyridamole (DPY). C) Rationale for combined DHODH and salvage pathway inhibition.

Aesar/Fisher (AAA1522706) for the NTP and antiviral assays, respectively.

2.2. Cell lines and virus

A549/ACE2 and HEK-293T-hACE2 (BEI resources, NR-53821 and NR-52511) cells were cultured in DMEM medium supplemented with 10% FBS and 2 mM L-glutamine. Cells were passed twice in a week and maintained at 37 °C with 5% CO₂. The absence of mycoplasma contamination was validated with a PCR-based method (ATCC, Universal Mycoplasma Detection Kit, 30–1012K). For antiviral experiments, A549 cells (ATCC CCL-185) were transduced with ACE2 lentivirus made using pLEX307-ACE2-puro (Addgene plasmid #158448), pLP1, pLP2, and pLP/VSV-G. Transduced cells were put under puromycin selection, then sorted by FACS into four bins based on ACE2 expression. See Supplemental Methods for details. The cell pool that gave optimal infection with minimal syncytia was used in assays.

2.3. In vitro determination of BRQ + DPY effect on pyrimidine NTPs

Cells were plated in 6-well plates (200,000 cells/well) one day prior to experiment. Test compounds were dissolved in DMSO as a stock and then diluted in culture medium before testing. The final concentration of DMSO was kept at 0.25%. For drug treatment, cell supernatant was removed and replaced with medium containing test compounds (n = 3 per group). At timepoints denoted, cell lysates were prepared according to a protocol published (Rodriguez et al., 2000) with minor modifications. In brief, cells were washed with PBS and treated with 0.75 mL of 0.4 N perchloric acid (PCA) on ice and harvested. Extracts were centrifuged (1500 rpm) and supernatants were combined with a second 0.25 mL extraction. Extracts were combined and neutralized with 10 N and 1 N KOH. Neutralization was determined using pH paper. Samples were stored at –20 °C. The NTP concentrations of samples were analyzed with HPLC.

PCA extracts were analyzed using either a Waters 2695e HPLC with a Waters 2489 UV/Visible detector or a Waters 2695 HPLC with a Waters 2487 Dual λ Absorbance detector. A Partisil 10 SAX column separated nucleoside triphosphates at a flow rate of 1.5 mL/min with a 50-min concave gradient curve (curve 8) from 60% 0.005 M NH₄H₂PO₄ (pH 2.8) and 40% 0.75 M NH₄H₂PO₄ (pH 3.8) to 100% 0.75 M NH₄H₂PO₄ (pH 3.8). Standard ribonucleotides were used to create a standard curve, which was used to quantitate nucleotide pools (Rodriguez et al., 2000).

Analysis of Variance with Dunnett's Multiple Comparisons Test was used to test for significant differences from the DMSO Control at Time 0 vs all other conditions or DMSO vs BRQ, DPY, or BRQ + DPY treatment at each timepoint (Supplemental Tables S3 and S4).

For assessment of cytotoxicity, cells were plated in white 96-well plates (18,000 cells/well) and cultured overnight. The next day, test compound diluted in cell culture medium were added to the cells at the final concentration (0.4–25 μM, 7 points by 2-fold serial dilution). After two days of incubation, cell viability was evaluated with CellTiter-Glo, measuring luminescence or Alamar-Blue (Ex 564/Em 600) with Synergy 4 (Biotek). 1% of Triton-X100 and 0.25% DMSO were 0 and 100% cell viability, respectively.

2.4. BRQ + DPY antiviral experiments

A549/ACE2 cells were plated in 96-well plates (10,000 cells/well) in RPMI supplemented with 10% FBS and allowed to adhere overnight. The following day cells were treated with 2-fold dilution series in triplicate of BRQ (0.0781–5 μM) and DPY (0.195–50 μM) in a matrix format allowing each concentration pair to be tested. Dilution series of each compound alone were included on each plate, as well as 10 μM remdesivir positive control and DMSO negative control wells. Exogenous uridine (20 μM) was added to an additional three plates to test whether BRQ inhibition of DHODH-catalyzed uridine synthesis can be

overcome by addition of excess uridine. Following 1 h of incubation with compounds, cells were challenged with approximately 400 FFU of SARS-CoV-2 Beta (B.1.351; hCoV-19/USA/MD-HP01542/2021) and incubated at 37 °C for 48 h. In a separate experiment using A549/ACE2 cells, dilution series of BRQ and DPY alone or BRQ + 0.78 μM or 12.5 μM DPY were tested with the SARS-CoV-2 Delta VOC (B.1.617.2). Pre-treatment time, infection dose, and length of infection were the same as with Beta variant. Analysis of Variance with Dunnett's Multiple Comparisons Test was used to test for significant differences from the DMSO Control vs BRQ or BRQ + DPY treatment or between BRQ alone vs BRQ + DPY. The 50% effective concentrations (EC₅₀s) were calculated using a 4-parameter variable slope model (GraphPad Prism).

2.5. Immunofluorescence detection of SARS-CoV-2 infection efficiency

Following 48 h of infection plates were fixed in 10% formalin for at least 6 h before removal from the high containment laboratory. Plates were washed in PBS, permeabilized in 0.1% Triton X-100 for 15 min at room temperature and blocked in 3.5% BSA for at least 1 h at room temperature. To detect infection, plates were incubated overnight at 4 °C with a rabbit anti-N protein monoclonal antibody (SioBiological 40143-R004) diluted 1:20,000. Plates were washed and treated with an AF488-conjugated goat anti-rabbit secondary antibody for 2 h at room temperature. Finally, Hoechst33342 was added to visualize cell nuclei. Plates were imaged on a Cytation 1 Multimode Plate Reader (BioTek) using a 4X objective lens. Infection efficiency, defined as GFP-positive cells divided by total nuclei, was calculated for each image using a CellProfiler pipeline.

2.6. Synergy calculations

Drug synergy was calculated with SynergyFinder2.0 (Ianevski et al., 2021) using inhibition readout, LL4 curve fitting, and ZIP model parameters.

2.7. MTT cell viability assay in uninfected A549/ACE2 cells

Cytotoxicity was assessed using the Roche MTT cell proliferation kit (Millipore Sigma 11465007001) with dilution series of brequinar and dipyradamole alone and at synergistic combinations, as determined from the synergy analysis (Fig. 4E and F). Briefly, A549/ACE2 cells were plated in 96-well plates at a density of 10,000 cells per well in 75 μL RPMI+10% FBS and allowed to attach overnight. The following day, 2-fold dilution series of brequinar (ranging 5 μM–0.0781 μM) and dipyradamole (ranging 50 μM–0.195 μM), and brequinar dose titrations with 12.5 μM or 0.78 μM dipyradamole were added to cells; each was tested in triplicate. Staurosporine ranging from 25 μM–0.0488 μM served as a positive cytotoxic control and DMSO as vehicle control. Following a 40-h incubation at 37 °C, MTT labeling reagent was added at a final concentration of 0.5 mg/mL and plates were incubated for 4 h at 37 °C, followed by addition of 100 μL solubilization reagent. After a final 1-h incubation, plates were read on a Tecan Spark microplate reader with measurements acquired at 575 nm and a reference wavelength of 675 nm.

3. Results

3.1. DPY potentiates the suppression of pyrimidine NTPs by BRQ without apparent cytotoxicity

Uninfected A549/ACE2 cells were treated with BRQ, DPY, or in combination (BRQ + DPY), over an 8-h time course. The concentration of cellular pyrimidine nucleotides (CTP and UTP) was measured and compared to control cells (T = 0, DMSO treated) (Fig. 2; Supplemental Table S1).

Purine nucleotide (ATP and GTP) concentrations were not decreased

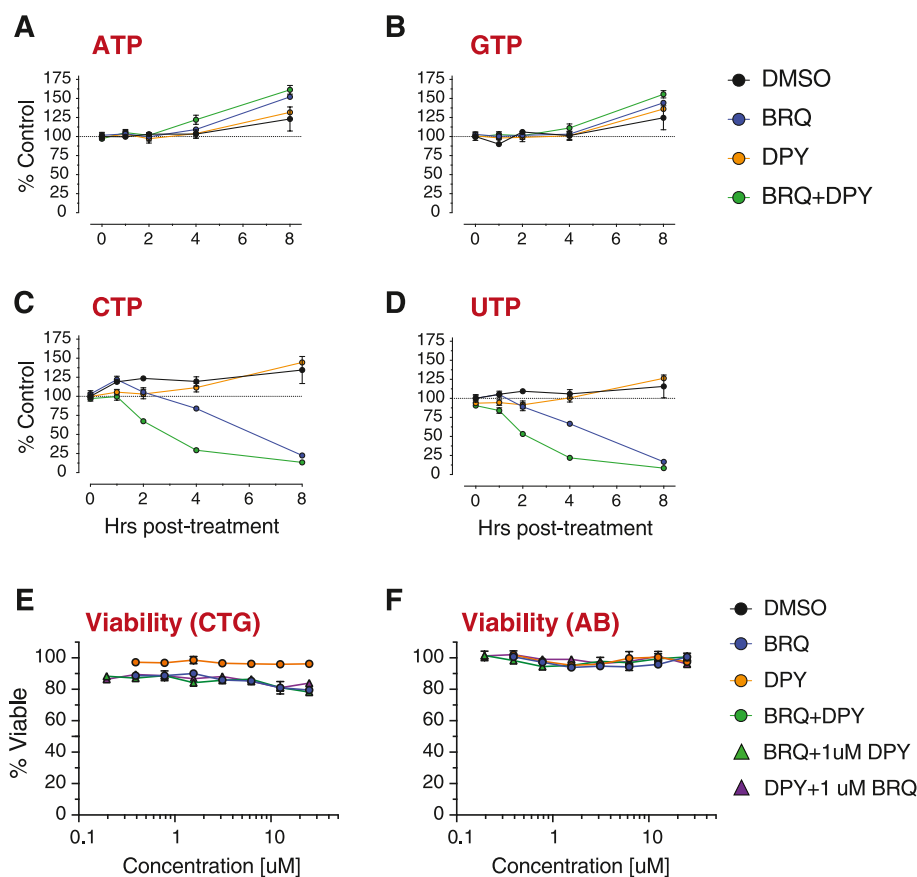


Fig. 2. DPY potentiates the suppression of pyrimidine NTPs by BRQ without cytotoxicity. A-D) Cellular nucleotide pools following treatment over 8 h with BRQ, DPY, or BRQ + DPY at 1 μ M each. Free NTP concentrations were normalized to the vehicle control group at 0 h post-treatment (n = 3 per time point, per group). A549/ACE2 cell viability was assessed with Cell-Titer Glo (E) or Alamar-Blue (F) following treatment with BRQ and/or DPY for two days with N = 3 wells for single agent treatment and N = 2 for combinations.

by any of the treatments (Fig. 2A–B). DPY alone (1 μ M) had no impact on UTP or CTP levels. BRQ alone (1 μ M) exhibited a reduction in pyrimidine NTPs (CTP and UTP) concentrations starting at 4 h (–16% and –33% for CTP and UTP, respectively) and the effect was more pronounced at 8 h (–77% and –83% for CTP and UTP, respectively) (Fig. 2C–D). The combination of BRQ + DPY (1 μ M each) demonstrated a potentiated effect. At 2 h, BRQ + DPY reduced CTP and UTP by 34% and 47%, respectively. At 4 h, BRQ + DPY reduced CTP and UTP concentrations by 71% and 79%, respectively. At 8 h, BRQ + DPY reduced CTP and UTP concentrations by 87% and 92%, respectively. The effect of combined BRQ + DPY on pyrimidine NTP levels was significant relative to controls and to single agent BRQ (Fig. 2; Supplemental Tables S3 and S4).

The effect of BRQ + DPY on pyrimidine NTP concentrations was not driven by general cytotoxicity as the CC₅₀ values for BRQ, DPY, or BRQ + DPY were >25 μ M even after two days of exposure (Fig. 2E and F;

Supplemental Table S2). Notably, these concentrations of BRQ and DPY are 10-fold higher than those used to assay the inhibition of pyrimidine biosynthesis and nucleoside salvage.

3.2. BRQ + DPY suppresses pyrimidine nucleotides even with high exogenous uridine

As DPY acts as a nucleoside transport inhibitor, we hypothesized that it could potentiate the BRQ-mediated decrease in pyrimidine NTP concentrations even in the presence of excess exogenous uridine. NTP concentrations were measured in the presence or absence of uridine (20 μ M) at 4 h post compound addition in HEK-293T-hACE2 (Fig. 3A) and A549/ACE2 cells (Fig. 3B). Pyrimidine NTP levels were substantially reduced with single agent BRQ (1 μ M): HEK-293T-hACE2 (–88% and –94% for CTP and UTP, respectively) and A549/ACE2 (–56% and –63% for CTP and UTP, respectively) cells. BRQ + DPY (1 μ M each)

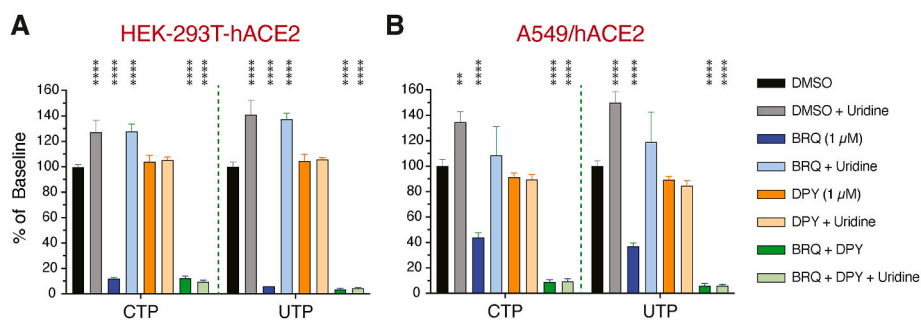


Fig. 3. BRQ + DPY suppresses levels of pyrimidine nucleotides even in presence of high concentrations of exogenous uridine. Pyrimidine NTP concentrations in HEK-293T-hACE2 (A) and A549/ACE2 (B) at 4 h post addition of BRQ, DPY and BRQ + DPY (1 μ M each) with/without 20 μ M uridine. Purine nucleotides levels were unaffected in either cell type (data not shown). **p < 0.01; ****p < 0.0001.

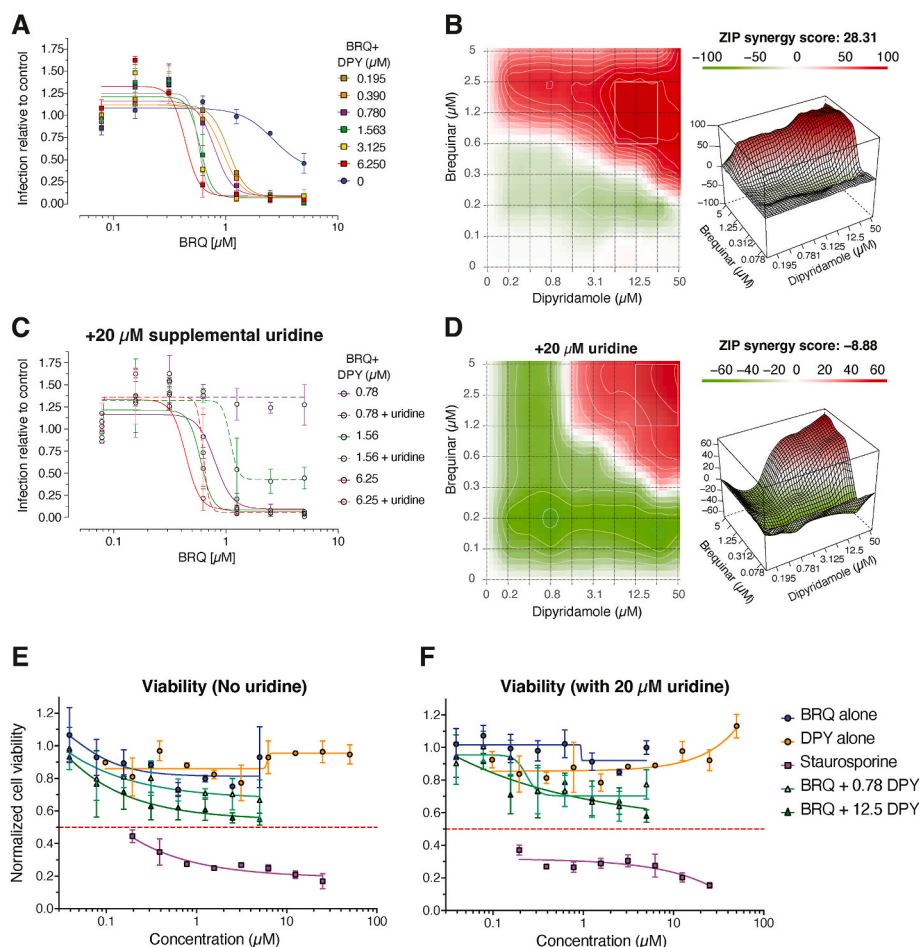


Fig. 4. BRQ + DPY exhibits strong synergistic antiviral activity that is partially abrogated by supplementation of extracellular uridine. The antiviral activity of BRQ + DPY was evaluated against SARS-CoV-2 Beta (B.1.351) in A549/ACE2 cells. **A)** Antiviral activity of BRQ (0.078–5.0 μM) alone or in combination with DPY (0.195–50.0 μM). **B)** Synergistic antiviral activity of BRQ + DPY using a combination of Loewe and Bliss models (Ianevski et al., 2021). **C)** Effect of excess exogenous uridine on BRQ + DPY antiviral activity; representative curves with/without uridine. **D)** Additive antiviral activity of BRQ + DPY using a combination of Loewe and Bliss models (Ianevski et al., 2021). Normalized uninfected A549/ACE2 cell viability assessed by MTT assay as described after 44 h post-compound addition without **(E)** or with **(F)** 20 μM uridine.

exhibited greater reduction of pyrimidine NTP levels than BRQ alone in both HEK-293T-hACE2 (–87% and –96% for CTP and UTP, respectively) and A549/ACE2 (–91% and –94% for CTP and UTP, respectively) cells; the latter consistent with the data in Fig. 2. Notably, in the presence of excess extracellular uridine, CTP and UTP levels remained stable in cells despite treatment with BRQ but not in cells treated with BRQ + DPY. Purine NTP levels were not impacted by BRQ or DPY or the combination (data not shown).

3.3. BRQ + DPY exhibits synergistic antiviral activity in vitro against SARS-CoV-2

As BRQ + DPY rapidly depleted the pyrimidine NTP pools required for viral RNA synthesis/replication (Fig. 2), we explored whether this combination exhibits enhanced antiviral activity compared to either agent alone.

3.3.1. BRQ + DPY demonstrates synergistic antiviral activity

BRQ + DPY was assessed in A549/ACE2 cells infected with SARS-CoV-2 Beta variant (B.1.351) (Fig. 4). DPY had no impact on SARS-CoV-2 infection (Supplemental Figure S1). The antiviral activity of BRQ was enhanced in a dose-dependent manner by the addition of pharmacologically relevant concentrations of DPY (Fig. 4A and Table 1) (Gregov et al., 1987). The EC₅₀ decreased from 2.67 μM for BRQ alone to 0.80 μM (3.3-fold lower), 0.59 μM (4.5-fold lower), and 0.44 μM (6.1-fold lower) in the presence of 0.78, 1.56, and 6.25 μM DPY, respectively. DPY alone does not exhibit antiviral activity at concentrations up to 50 μM (Supplemental Figure S1). Similar enhancement of BRQ antiviral activity with the addition of DPY was also observed in

Table 1
BRQ + DPY Synergy vs SARS-CoV-2 Beta (B.1.351).

| Treatment | EC ₅₀ [μM] No Added Uridine | Fold-Change vs BRQ Alone | EC ₅₀ [μM] With 20 μM Uridine | Fold-Change vs BRQ Without Added Uridine |
|--|--|--------------------------|--|--|
| DPY Alone | >50 | N/A | >50 | N/A |
| BRQ Alone | 2.67 | 1.00 | >5 | >1.87 |
| BRQ + 0.195 μM DPY | 1.06 | –2.51 | >5 | >4.70 |
| BRQ + 0.390 μM DPY | 0.94 | –2.85 | >5 | >5.34 |
| BRQ + 0.789 μM DPY | 0.80 | –3.35 | >5 | >6.27 |
| BRQ + 1.563 μM DPY | 0.59 | –4.50 | 1.09 | 1.84 |
| BRQ + 3.125 μM DPY | 0.57 | –4.66 | 0.90 | 1.57 |
| BRQ + 6.250 μM DPY | 0.44 | –6.12 | 0.63 | 1.44 |
| BRQ + 12.5 μM DPY | 0.32 | –8.24 | 0.40 | 1.23 |
| BRQ + 25 μM DPY | 0.28 | –9.48 | 0.28 | 1.00 |
| BRQ + 50 μM DPY | 0.28 | –9.53 | 0.27 | 1.00 |
| Synergy Score (Ave)^a | 22.57 | Synergy | –4.66 | Additivity |

^a Determined with ZIP (Bliss + Loewe); Synergy scores (Average of three technical replicates): >10.0 indicates synergy; –10 to 10 indicates additivity; < –10 indicates antagonism; N/A: Not Applicable.

Vero cells infected with geographically distinct Wuhan-related SARS-CoV-2 strains (Supplemental Figures S2A and S3A). The cytotoxicity of BRQ, DPY, or BRQ + DPY ranged from <10% to <50% by 5 different methodologies (Fig. 2E, F, 4E and 4F; Supplemental Figures S2B and S3B).

BRQ + DPY exhibited a strong synergistic interaction (Fig. 4B and Table 1), including at pharmacologically relevant drug concentrations. The average synergy score from three replicates was 22.6, with the most synergistic area covering 75.2 arbitrary square units.

3.3.2. Exogenous uridine supplementation partially abrogates the synergistic effect

The effect of excess exogenous uridine on the antiviral activity of BRQ + DPY was more pronounced at DPY concentrations <3 μM where substantial or complete reversal of antiviral activity (e.g., EC_{50} > maximum concentration tested) was observed. DPY concentrations at or above 6.25 μM decreased the impact of excess uridine (Table 1, examples in Fig. 4C). Consistent with the increase in EC_{50} values for BRQ + DPY in the presence of 20 μM uridine, synergy analysis of infection data revealed a shift in synergistic dose combinations to higher concentrations of both drugs (Fig. 4D). Furthermore, the synergy score in the presence of excess exogenous uridine was -4.7. This score, indicative of an additive interaction, was confounded by the apparent antagonism of excess uridine at low concentrations of DPY and by the lesser effect at higher DPY concentrations. The physiological relevance of 20 μM uridine, which is 2- to 9-fold higher than physiologic levels (Karle et al., 1980), has not been determined.

3.3.3. BRQ antiviral activity against SARS-CoV-2 Delta variant of concern (B.1.617.2) is enhanced with low concentrations of DPY

Based on the findings with SARS-CoV-2 Beta (B.1.351), the antiviral activity of BRQ + DPY was evaluated in the same assay system using the SARS-CoV-2 Delta variant of concern (VOC) (B.1.617.2) (Fig. 5). BRQ + DPY also exhibited enhanced antiviral activity against SARS-CoV-2 Delta (B.1.617.2), relative to DMSO control as well as to BRQ alone.

4. Discussion

There remains a significant need for safe and convenient treatments for COVID-19 especially as recently authorized antivirals have challenges with pill burden, inconvenient routes of administration, or potential drug interactions. While the clinical efficacy of DHODHI antiviral monotherapy remains to be proven, clinical experience in the oncology

space suggests that extracellular uridine and the activity of nucleoside transporters may limit the efficacy of DHODHI monotherapy. Given the growing evidence suggesting that DHODH inhibition alone *in vitro* may not translate to *in vivo* activity, we explored a host-target antiviral strategy with the combination BRQ and DPY.

DPY enhanced the inhibitory effect of BRQ on the concentration of intracellular pyrimidine NTPs *in vitro* in HEK-293T-hACE2 and A549/ACE2 cell lines. Depletion of pyrimidine NTP pools by BRQ could be overcome with the addition of excess exogenous uridine (20 μM) whereas the inhibitory activity of BRQ + DPY was preserved. Furthermore, the inhibitory activity associated with low concentrations of BRQ and DPY was not driven by apparent cytotoxicity.

Viral RNA transcripts comprise more than 50% of RNA transcripts in SARS-CoV-2 infected cells and all nucleotides are host-derived (Kim et al., 2020). DPY or BRQ as single agents exhibited no to marginal single agent antiviral activity, respectively, against SARS-CoV-2 consistent with published reports (Calistri et al., 2021; Schultz et al., 2022; Xiong et al., 2020) and Clear Creek Bio data (not shown). As hypothesized, BRQ + DPY exhibited strong, synergistic antiviral activity beyond that of BRQ alone; this was evident at concentrations with potential pharmacologic relevance, (<2 μM each (Clear Creek Bio data on file; Gregov et al., 1987; Joshi et al., 1997)), was not driven by apparent cytotoxicity even at high concentrations and was not reversed in the presence of excess exogenous uridine. These data support the concept that inhibiting both *de novo* and salvage pyrimidine pathways with BRQ + DPY merits further exploration.

A major area of concern is the development of viral resistance, via selective pressures by DAAs, or viral immune escape with the emergence of novel SARS-CoV-2 VOCs observed after vaccination and the development of natural immunity. As BRQ and DPY target host proteins, the inability of excess exogenous uridine to reverse the BRQ + DPY effects on pyrimidine depletion and the antiviral activity against different SARS-CoV-2 strains and variants, suggests this combination has a reduced likelihood for the development of resistance.

Given our *in vitro* results, a similar synergy and enhancement of BRQ antiviral activity may be observed *in vivo* by combination with DPY. As this combination has not been previously used as an antiviral treatment, a careful clinical assessment of the safety of this combination in patients needs to be performed prior to larger scale efficacy clinical trials. It is assuring that there is a well-established safety profile for chronic use of both BRQ and DPY. As the initial step to safely evaluate the antiviral activity of this combination in COVID-19 patients, a small dose escalation safety study was initiated in India in late 2021 (CCB-CRISIS-04.,

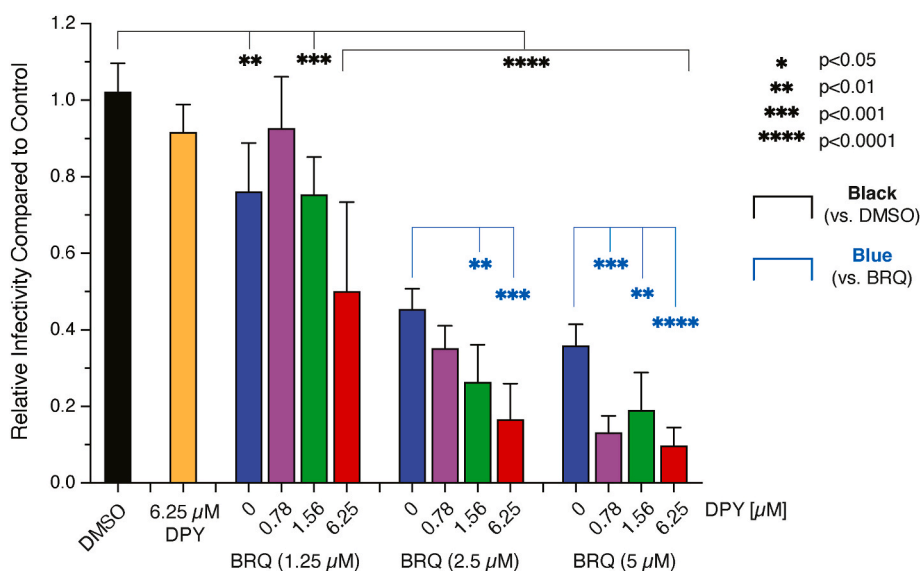


Fig. 5. Dose-dependent enhancement of BRQ antiviral activity against SARS-CoV-2 Delta VOC (B.1.617.2) with low concentrations of DPY. Informed by the data in Figures S1 and 4, the antiviral activity of BRQ alone (1.25, 2.5 and 5.0 μM) or in combination with DPY (0.78, 1.56, and 6.25 μM) was evaluated against SARS-CoV-2 Delta VOC (B.1.617.2) in A549/ACE2 cells. ANOVA with Dunnett's Multiple Comparisons Test was used to test for significant differences from the DMSO Control vs BRQ or BRQ + DPY treatment or between BRQ alone vs BRQ + DPY.

2022, NCT05166876). Unfortunately, the trial had to be terminated early for insufficient enrollment due to declining incidence of COVID-19 in India. A new clinical trial is currently being planned. Ultimately, if this approach is successful, investigation of the use of BRQ + DPY in other RNA viral infections may be warranted.

Declaration of competing interest

The authors declare that they have no known competing financial interests or personal relationships that could have appeared to influence the work reported in this paper.

Acknowledgements

The following reagent was obtained through BEI Resources, NIAID, NIH: Human Lung Carcinoma Cells (A549) Expressing Human Angiotensin-Converting Enzyme 2, NR-53821, and Human Embryonic Kidney Cells (HEK-293T) Expressing Human Angiotensin-Converting Enzyme 2, HEK-293T-hACE2 Cell Line, NR-52511). We thank Dr. Olga Kharchenko for assistance with Fig. 1. J.F.D, M.K, J.C.P. Jr, N.S., D.B.S., and V.K. own stock in Clear Creek Bio. V.G. and D.C are paid consultants of Clear Creek Bio. Clear Creek Bio funded all work described in this article, including Sponsored Research Agreements with Boston University, MD Anderson Cancer Center, and the University of Louisville.

Appendix A. Supplementary data

Supplementary data related to this article can be found at <https://doi.org/10.1016/j.antiviral.2022.105403>.

References

- Adcock, R.S., Chu, Y.-K., Golden, J.E., Chung, D.-H., 2017. Evaluation of anti-Zika virus activities of broad-spectrum antivirals and NIH clinical collection compounds using a cell-based, high-throughput screen assay. *Antivir. Res.* 138, 47–56. <https://doi.org/10.1016/j.antiviral.2016.11.018>.
- Aggrenox®, U.S.P.I., 2012. Highlights of Prescribing Information for AGGRENOX® (Aspirin/extended-release Dipyridamole) Capsules Initial US Approval 1999 accessed 20May2022). https://www.accessdata.fda.gov/drugsatfda_docs/label/2012/020884s030lbl.pdf.
- Bonavia, A., Franti, M., Pusateri Keane, E., Kuhen, K., Seepersaud, M., Radetich, B., Shao, J., Honda, A., Dewhurst, J., Balabanis, K., Monroe, J., Wolff, K., Osborne, C., Lanieri, L., Hoffmaster, K., Amin, J., Markovits, J., Broome, M., Skuba, E., Cornella-Taracido, I., Joberty, G., Bouwmeester, T., Hamann, L., Tallarico, J.A., Tommasi, R., Compton, T., Bushell, S.M., 2011. Identification of broad-spectrum antiviral compounds and assessment of the druggability of their target for efficacy against respiratory syncytial virus (RSV). *Proc. Natl. Acad. Sci. USA* 108, 6739–6744. <https://doi.org/10.1073/pnas.1017142108>.
- Calistri, A., Luginani, A., Mognetti, B., Elder, E., Sibille, G., Conciatori, V., del Vecchio, C., Sainas, S., Boschi, D., Montserrat, N., Mirazimi, A., Lollì, M.L., Gribaudo, G., Parolin, C., 2021. The new generation hDHODH inhibitor MEDS433 hinders the in vitro replication of SARS-CoV-2 and other human coronaviruses. *Microorganisms* 9, 1731. <https://doi.org/10.3390/microorganisms9081731>.
- CCB-CRISIS-04, 2022. Brequinar Combined With Dipyridamole in Patients With Mild to Moderate COVID-19 (CCBCRISIS04). <https://clinicaltrials.gov/ct2/show/NCT05166876>. (Accessed 20 May 2022).
- Cuthbertson, C.R., Guo, H., Kyani, A., Madak, J.T., Arabzade, Z., Neamati, N., 2020. The dihydroorotate dehydrogenase inhibitor brequinar is synergistic with ENT1/2 inhibitors. *ACS Pharmacol. Transl. Sci.* 3, 1242–1252. <https://doi.org/10.1021/acspetsci.0c00124>.
- FDA, 2022. Drugs@FDA: FDA-Approved Drugs. New Drug Application #012836 Persantine (dipyridamole). In: <https://www.accessdata.fda.gov/scripts/cder/da/f/index.cfm?event=overview.process&AppNo=012836>. (Accessed 20 May 2022).
- Gregov, D., Jenkins, A., Duncan, E., Siebert, D., Rodgers, S., Duncan, B., Bochner, F., Lloyd, J., 1987. Dipyridamole: pharmacokinetics and effects on aspects of platelet function in man. *Br. J. Clin. Pharmacol.* 24, 425–434. <https://doi.org/10.1111/j.1365-2125.1987.tb03194.x>.
- Ianevski, A., Giri, A.K., Aittokallio, T., 2021. SynergyFinder 2.0: visual analytics of multi-drug combination synergies. *Nucleic Acids Res.* 48, W488–W493. <https://doi.org/10.1093/NAR/GKAA216>.
- Joshi, A.S., King, S.-Y.P., Zajac, B.A., Makowka, L., Sher, L.S., Kahan, B.D., Menkis, A.H., Stillier, C.R., Schaeffe, B., Kornhauser, D.M., 1997. Phase I safety and pharmacokinetic studies of brequinar sodium after single ascending oral doses in stable renal, hepatic, and cardiac allograft recipients. *J. Clin. Pharmacol.* 37, 1121–1128. <https://doi.org/10.1002/j.1552-4604.1997.tb04296.x>.
- Karle, J.M., Anderson, L.W., Dietrick, D.D., Cysyk, R.L., 1980. Determination of serum and plasma uridine levels in mice, rats, and humans by high-resolution liquid chromatography. *Anal. Biochem.* 109, 41–46. [https://doi.org/10.1016/0003-2697\(80\)90007-X](https://doi.org/10.1016/0003-2697(80)90007-X).
- Kim, Y.-J., Cubitt, B., Cai, Y., Kuhn, J.H., Vitt, D., Kohlfhof, H., de la Torre, J.C., 2020. Novel dihydroorotate dehydrogenase inhibitors with potent interferon-independent antiviral activity against mammarenaviruses in vitro. *Viruses* 12, 821. <https://doi.org/10.3390/v12080821>.
- Liu, Q., Gupta, A., Okesli-Armlovich, A., Qiao, W., Fischer, C.R., Smith, M., Carette, J.E., Bassik, M.C., Khosla, C., 2020. Enhancing the antiviral efficacy of RNA-dependent RNA polymerase inhibition by combination with modulators of pyrimidine metabolism. *Cell Chem. Biol.* 27, 668–677. <https://doi.org/10.1016/j.chembiol.2020.05.002> e9.
- Madak, J.T., Bankhead, A., Cuthbertson, C.R., Showalter, H.D., Neamati, N., 2019. Revisiting the role of dihydroorotate dehydrogenase as a therapeutic target for cancer. *Pharmacol. Therapeut.* 195, 111–131. <https://doi.org/10.1016/j.pharmthera.2018.10.012>.
- Park, J.-G., Ávila-Pérez, G., Nogales, A., Blanco-Lobo, P., de la Torre, J.C., Martínez-Sobrido, L., 2020. Identification and characterization of novel compounds with broad-spectrum antiviral activity against influenza A and B viruses. *J. Virol.* 94. <https://doi.org/10.1128/JVI.02149-19>.
- Peters, G., Kraal, L., Pinedo, H., 1992. In vitro and in vivo studies on the combination of Brequinar sodium (DUP-785; NSC 368390) with 5-fluorouracil; effects of uridine. *Br. J. Cancer* 65, 229–233. <https://doi.org/10.1038/bjc.1992.46>.
- Peters, G.J., Schwartzmann, G., Nadal, J.C., Laurens, E.J., van Groeningen, C.J., van der Vijgh, W.J., Pinedo, H.M., 1990. In vivo inhibition of the pyrimidine de novo enzyme dihydroorotic acid dehydrogenase by brequinar sodium (DUP-785; NSC 368390) in mice and patients. *Cancer Res.* 50, 4644–4649.
- Qing, M., Zou, G., Wang, Q.-Y., Xu, H.Y., Dong, H., Yuan, Z., Shi, P.-Y., 2010. Characterization of Dengue virus resistance to brequinar in cell culture. *Antimicrob. Agents Chemother.* 54, 3686–3695. <https://doi.org/10.1128/AAC.00561-10>.
- Rodriguez, C.O., Plunkett, W., Paff, M.T., Du, M., Nowak, B., Ramakrishna, P., Keating, M.J., Gandhi, V., 2000. High-performance liquid chromatography method for the determination and quantitation of arabinosylguanine triphosphate and fludarabine triphosphate in human cells. *J. Chromatogr. B* 745, 421–430.
- Schultz, D.C., Johnson, R.M., Ayyanathan, K., Miller, J., Whig, K., Kamalia, B., Dittmar, M., Weston, S., Hammond, H.L., Dillen, C., Ardanuy, J., Taylor, L., Lee, J.S., Li, M., Lee, E., Shoffler, C., Petucci, C., Constant, S., Ferrer, M., Thaiss, C.A., Frieman, M.B., Cherry, S., 2022. Pyrimidine inhibitors synergize with nucleoside analogues to block SARS-CoV-2. *Nature* 604, 134–140. <https://doi.org/10.1038/s41586-022-04482-x>.
- Sykes, D.B., Kfoury, Y.S., Mercier, F.E., Wawer, M.J., Law, J.M., Haynes, M.K., Lewis, T.A., Schajnovitz, A., Jain, E., Lee, D., Meyer, H., Pierce, K.A., Tolliday, N.J., Waller, A., Ferrara, S.J., Eheim, A.L., Stoeckigt, D., Maxcy, K.L., Cobert, J.M., Bachand, J., Szekely, B.A., Mukherjee, S., Sklar, L.A., Kotz, J.D., Clish, C.B., Sadreyev, R.I., Clemons, P.A., Janzer, A., Schreiber, S.L., Scadden, D.T., 2016. Inhibition of dihydroorotate dehydrogenase overcomes differentiation blockade in acute myeloid leukemia. *Cell* 167, 171–186. <https://doi.org/10.1016/j.cell.2016.08.057> e15.
- Wang, H., Paulson, K.R., Pease, S.A., Watson, S., Comfort, H., Zheng, P., Aravkin, A.Y., Bisignano, C., Barber, R.M., Alam, T., Fuller, J.E., May, E.A., Jones, D.P., Frisch, M. E., Abbafati, C., Adolph, C., Allorant, A., Amlag, J.O., Bang-Jensen, B., Bertolacci, G. J., Bloom, S.S., Carter, A., Castro, E., Chakrabarti, S., Chattopadhyay, J., Cogen, R. M., Collins, J.K., Cooperider, K., Dai, X., Dangel, W.J., Daoud, F., Dapper, C., Deen, A., Duncan, B.B., Erickson, M., Ewald, S.B., Fedosseeva, T., Ferrari, A.J., Frostad, J.J., Fullman, N., Gallagher, J., Gamkrelidze, A., Guo, G., He, J., Helak, M., Henry, N.J., Hulland, E.N., Huntley, B.M., Kereselidze, M., Lazzarato, A., LeGrand, K.E., Lindstrom, A., Lineberger, E., Lotufo, P.A., Lozano, R., Magistro, B., Malta, D.C., Månsson, J., Mantilla Herrera, A.M., Marinho, F., Mirkuzie, A.H., Misganaw, A.T., Monasta, L., Naik, P., Nomura, S., O'Brien, E.G., O'Halloran, J.K., Olana, L.T., Ostroff, S.M., Penberthy, L., Reiner Jr, R.C., Reinke, G., Ribeiro, A.L.P., Santomauro, D.F., Schmidt, M.I., Shaw, D.H., Sheena, B.S., Sholokhov, A., Shkhvitaridze, N., Sorensen, R.J.D., Spurlock, E.E., Syailendrawati, R., Topor-Madry, R., Troeger, C.E., Walcott, R., Walker, A., Wiysonge, C.S., Worku, N.A., Zigler, B., Pigott, D.M., Naghavi, M., Mokdad, A.H., Lim, S.S., Hay, S.I., Gakidou, E., Murray, C.J.L., 2022. Estimating excess mortality due to the COVID-19 pandemic: a systematic analysis of COVID-19-related mortality, 2020–21. *Lancet* 399, 1513–1536. [https://doi.org/10.1016/S0140-6736\(21\)02796-3](https://doi.org/10.1016/S0140-6736(21)02796-3).
- Wang, Q.-Y., Bushell, S., Qing, M., Xu, H.Y., Bonavia, A., Nunes, S., Zhou, J., Poh, M.K., Florez de Sessions, P., Niyomrattanakit, P., Dong, H., Hoffmaster, K., Goh, A., Nilar, S., Schul, W., Jones, S., Kramer, L., Compton, T., Shi, P.-Y., 2011. Inhibition of Dengue virus through suppression of host pyrimidine biosynthesis. *J. Virol.* 85, 6548–6556. <https://doi.org/10.1128/JVI.02510-10>.
- WHO, 2022. WHO Coronavirus (COVID-19) Dashboard. <https://covid19.who.int/>. (Accessed 20 May 2022).
- Xiong, R., Zhang, L., Li, S., Sun, Y., Ding, M., Wang, Y., Zhao, Y., Wu, Y., Shang, W., Jiang, X., Shan, J., Shen, Z., Tong, Y., Xu, L., Chen, Y., Liu, Y., Zou, G., Lavillete, D., Zhao, Z., Wang, R., Zhu, L., Xiao, G., Lan, K., Li, H., Xu, K., 2020. Novel and potent inhibitors targeting DHODH are broad-spectrum antivirals against RNA viruses including newly-emerged coronavirus SARS-CoV-2. *Protein. Cell* 11, 723–739. <https://doi.org/10.1007/s13238-020-00768-w>.